

Article

Physical Modeling of the Stability of a Revetment Breakwater Built on Reclaimed Coral Calcareous Sand Foundation in the South China Sea—Regular Wave

Kunpeng He ^{1,2} and Jianhong Ye ^{1,*} 

¹ State Key Laboratory of Geomechanics and Geotechnical Engineering, Institute of Rock and Soil Mechanics, Chinese Academy of Sciences, Wuhan 430071, China; hekunpeng18@mails.ucas.ac.cn

² University of Chinese Academy of Sciences, Beijing 100049, China

* Correspondence: Jhye@whrsm.ac.cn

Abstract: In the past several years, a series of artificial islands have been constructed on the top of coral reefs by China in the South China Sea by way of reclamation. A large number of revetment breakwater also has been built along the margin of these artificial islands. The stability of these revetment breakwater is the precondition for the normal service performance of these reclaimed coral sand islands. In this study, taking the reclamation engineering in the South China Sea as the background, a series of wave flume physical model tests (geometrical similarity scale is set to 1:10) are performed to investigate the dynamics and the stability of the revetment breakwater and its reclaimed coral sand foundation under the impact of regular wave. Experimental results show that the revetment breakwater has a maximum final settlement of 6 mm if built on loose coral sand foundation. Furthermore, there is indeed excess pore pressure generated in the reclaimed coral foundation with a maximum magnitude of 1.5 kPa. It is found that the excess pore pressure has not caused liquefaction in the coral sand foundation due to the fact that the accumulation of excess pore pressure only occurred in the first 10 cycles of wave loading. Finally, it is concluded that the revetment breakwater and its reclaimed coral sand foundation basically are stable under regular wave impacting. However, excessive water overtopping would be a potential threat for the vegetation behind the breakwater, as well as for the desalinated underground water of the reclaimed lands.

Keywords: stability of breakwater; reclaimed coral sand foundation; South China Sea; regular wave; revetment breakwater; physical modeling



Citation: He, K.; Ye, J. Physical Modeling of the Stability of a Revetment Breakwater Built on Reclaimed Coral Calcareous Sand Foundation in the South China Sea—Regular Wave. *Appl. Sci.* **2021**, *11*, 2325. <https://doi.org/10.3390/app11052325>

Academic Editor: Cheng-Yu Ku

Received: 17 January 2021

Accepted: 1 March 2021

Published: 5 March 2021

Publisher's Note: MDPI stays neutral with regard to jurisdictional claims in published maps and institutional affiliations.



Copyright: © 2021 by the authors. Licensee MDPI, Basel, Switzerland. This article is an open access article distributed under the terms and conditions of the Creative Commons Attribution (CC BY) license (<https://creativecommons.org/licenses/by/4.0/>).

1. Introduction

The South China Sea is an important transport channel for the world trade and energy transportation. In order to conduct scientific research, ocean observation and to guarantee aviation safety and marine rescue, a series of artificial lands have been successfully built on the top of the coral reefs by way of reclamation of coral calcareous sand. A large number of revetment breakwaters have also been built along the outer margins of the reclaimed lands in order to avoid the direct erosion of the reclaimed artificial lands by ocean waves and enhance their stability. However, there were many instances of offshore structure failure under the great wave impact, for example, the breakwater in Lianyungang Port was seriously damaged by huge ocean waves in 1957 [1]. In 1994, the No. 3 drilling platform of Shengli oilfield in China collapsed due to the liquefaction that occurred in its seabed foundation under the impact of severe waves [2]. In 1976, the breakwater at Niigata Port, Japan, was severely damaged by a large storm wave [3]. Before the construction of the Mutriku Marine power station was completed, the breakwater was destroyed many times by severe storms from 2007 to 2009 [4]. Meteorological observation shows that tropical storms and typhoons are a frequent occurrence in the South China Sea. There are 2–3 severe typhoons and 5–6 tropical storms in the sea each year [5]. As a result, the artificial islands

in the South China Sea will be impacted frequently by huge waves in their service period. Stability of these revetment breakwaters is the precondition for the safety of the artificial islands in the South China Sea. Therefore, it is of great engineering significance to study the stability of the revetment breakwater in the South China Sea under the long-term impact of the extreme waves.

Many scholars have carried out a series of works on the stability of breakwater under the impact of ocean waves. Numerical analysis and physical model tests are mainly included. Remarkable progress has been made in the past 20 years on the aspect of numerical analysis. Many scholars have studied the stability of various types of breakwaters and the dynamic response of their seabed foundation by adopting elastoplastic finite element model developed by themselves or the commercial companies [6–13]. However, the deformable seabed foundation was often regarded as a permeable but rigid medium in these models. In order to overcome this shortcoming, Ye et al. [14,15] successfully developed an integrated numerical model FSSI-CAS 2D/3D, which can take fluid–structure–seabed interaction into consideration. This model has been successfully applied to study the dynamics of seabed foundation and the stability of breakwater in a practical project [16]. In addition to numerical methods, it is also of great significance to carry out physical model tests to study the stability of large-scale breakwater in important projects in which complex conditions are frequently involved.

A series of wave flume tests were carried out by many scholars to study the effect of different waveforms, in which regular and irregular waves were mainly involved [17–19]. These works have proved that regular waves would cause greater damage to breakwaters than random waves. It is noteworthy that Jensen [20] pointed out that the effect of the two kinds of waveform on breakwaters is basically the same if the wave height of regular waves is equal to the average value of the maximum 20 wave heights of irregular waves in a certain period of time. The conversion relations of wave impact on breakwaters induced by random waves and regular waves has also been deduced [21]. The effect of other wave parameters, such as wave period and water depth, has also been comprehensively studied [22–24]. The influence of different structure styles on the stability of breakwaters was studied by many scholars through laboratory wave flumes. Vicinanza et al. [25] found that the stability of breakwater would be significantly enhanced after the OBREC (Overtopping Breakwater for Energy Conversion) was installed. Christensen et al. [26] proved that the wing plate could restrict the movement of the floating breakwater, and the porous media on both sides of the wing plate could effectively reduce the reflection and transmission of ocean waves. The effect of accropode arrangement [27], seabed slope [28], parapet geometry [29], and toe berm geometry [30] on the stability of breakwater was also illustrated in detail by physical model test results. In addition, a systematic approach and relevant formulas were also proposed to evaluate the stability of breakwaters [31–34]. The above works have studied many factors affecting the stability of breakwater and successfully revealed the interaction between waves and breakwaters from the perspective of fluid dynamics. However, the plastic deformation and liquefaction of seabed foundation were not considered in them.

Currently, it has been widely recognized that there are three types of failure mode for the wave-induced failure of offshore breakwater. They are, respectively: (1) excessive residual horizontal displacement of breakwater due to slipping, referred to as model I; (2) breakwater is overturned due to huge wave impact, referred to as model II; (3) the foundation of breakwater partially or completely lost bearing capacity due to softening or liquefaction [35–37], referred to as model III. Due to the fact that the seabed foundation of breakwater was not, or could not be, taken into consideration in numerical computation or physical model test, the safety of breakwater can be only checked for the failure mode I and failure mode II in most previous works or some currently implemented national design codes, e.g., the Chinese code of design and construction of breakwater [38] or the Ocean Engineering Handbook [39]. Actually, the wave, breakwater and its foundation are a coupled system in the ocean environment. The foundation of breakwater plays an

important role in guaranteeing the stability of breakwater. Engineering case survey for breakwater failure shows that about 60–70% of failure cases have a closed relationship with the softening and liquefaction of foundation soil due to the pore pressure accumulation under cyclic wave loading. Therefore, the evaluation for the safety of breakwater is not reliable if the foundation of breakwater is not taken into consideration, regardless of adopting numerical modeling or physical model test.

In this study, taking the reclamation engineering in the South China Sea as the engineering background, a series of large-scale physical model tests are carried out to study the dynamics and the stability of the revetment breakwater built on the reclaimed coral sand foundation under extreme regular wave impacting. The physical model is established in a wave flume by a geometrical scale of 1:10. It is found that the revetment breakwater does have a certain settlement under the impacting of extreme wave loading and finally reaches a stable state. In addition, it is worth noting that the ability of the revetment breakwater against overtopping is relatively weak. The testing results can be a solid basis for the further works and provide some valuable references for the design as well as the past-construction maintenance of the revetment breakwaters built on the reclaimed coral reef islands in the South China Sea.

2. Experimental Setup

The dimension of the wave flume used in this study is 50.0 m in length, 1.3 m in height and 1.0 m in width. Due to the limited height of the wave flume, it is impossible to physically simulate the overall slope of the natural coral reef which generally is up to several thousand meters high in ocean. A possible approach is to focus only on the interaction between the wave on reef flat and the revetment breakwater as well as its reclaimed coral sand foundation, to observe the displacement of the breakwater, settlement and deformation of the reclaimed coral sand foundation under the impacting of ocean waves [40]. Therefore, the physical model in the wave flume only includes the revetment breakwater, coral calcareous sand foundation and the reef flat in this study.

The physical model is constructed according to a geometric similarity scale of 1:10. The schematic map of the physical model constructed in the wave flume is illustrated in Figure 1. In the physical model, the revetment breakwater consists of two parts, a revetment and a vertical caisson. Both parts of the revetment breakwater are made of concrete. For the sake of simplicity, the revetment is referred to as structure A, and the vertical caisson is referred to as structure B in the following analysis. The foundation behind and below the breakwater is built with coral calcareous sand over the original calcareous deposits on the top of natural reefs, which is modeled by a sand–gravel mixture in the physical model. In the engineering of practice, the revetment breakwater is usually covered by a great number of armor blocks such as accropodes and rocks to dissipate the wave energy. Correspondingly, some small accropodes also have been made and are laid on the revetment breakwater in the physical model, as shown in Figure 1. Hydrological parameters are determined based on the long-term observation in the South China Sea in the past 20 years. The elevation of extreme high-water level is set as +2.3 m above the average sea level ± 0 m in the design of the practical engineering. According to the distance from the water level to the vertical caisson, and applying the geometrical similarity scale 1:10, the water depth in the wave flume for the extreme high-water level and average water level is determined as 0.71 m and 0.48 m, respectively, in the physical model tests.

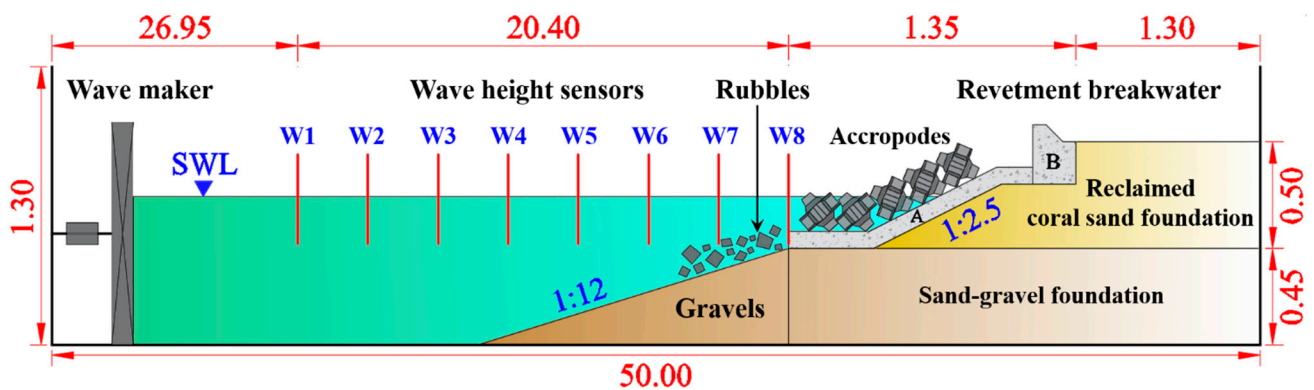


Figure 1. Schematic map of the physical model constructed in the wave flume (unit: m) (the revetment is labelled as A, and the vertical caisson is labelled as B).

The distance from the left side of the revetment breakwater to the wave maker is about 47.25 m. Eight wave profile sensors labelled as W1 to W8 are installed at typical positions in the wave flume. The locations of these wave profile sensors are listed in Table 1. The revetment breakwater and accropode model is made of C50 concrete, which is the same as that used in-site. The reclaimed foundation is made adopting coral calcareous sand sampled from a reclaimed coral reef island in the South China Sea. The original soil layer beneath the reclaimed coral calcareous sand foundation is modeled with a mixture of quartz sand and gravels. The mass ratio of quartz sand to gravel is set as 1.6:1, ensuring that the permeability coefficient of the mixture is close to that of the original soil layer. Gravels with a particle size of 1–2 cm are used to model the reef flat in front of the revetment breakwater. It is worthy to note that the real micro-topography of reef flat is complicated (uneven and rough). It has significant effect on the wave propagation and the wave energy dissipation. However, the complicated micro-topography of reef flat is impossible to be reproduced accurately in the physical model test. The upper surface of the gravel in the physical model is rough and uneven, which could simulate the reef flat in aspect of absorbing wave energy to some extent. The mechanical parameters of the materials used in physical model are listed in Table 2.

Table 1. Location of the wave profile sensors (distance to the wave maker).

Sensor No.	W1	W2	W3	W4	W5	W6	W7	W8
Location (m)	26.95	29.95	32.95	35.95	38.95	41.95	44.67	47.35

Table 2. Mechanical parameters of the materials used in the physical model.

Material	Elasticity Modulus (MPa)	Permeability (m/s)	D50 (mm)
Concrete	450	0	-
Calcareous Sand	30	2.0×10^{-5}	0.54
Sand-Gravel	50	6.8×10^{-4}	2
Gravel	80	1.0×10^{-1}	15

There are 14 pore pressure sensors buried in the reclaimed coral sand foundation, and there are another three pore pressure sensors buried in the sand-gravel mixture layer. There are, in total, 23 pressure sensors which are uniformly installed on the surface of structure A and B. Two LVDTs (Linear Variable Differential Transformer) are installed horizontally and vertically on the top of structure B, as shown in Figure 2.

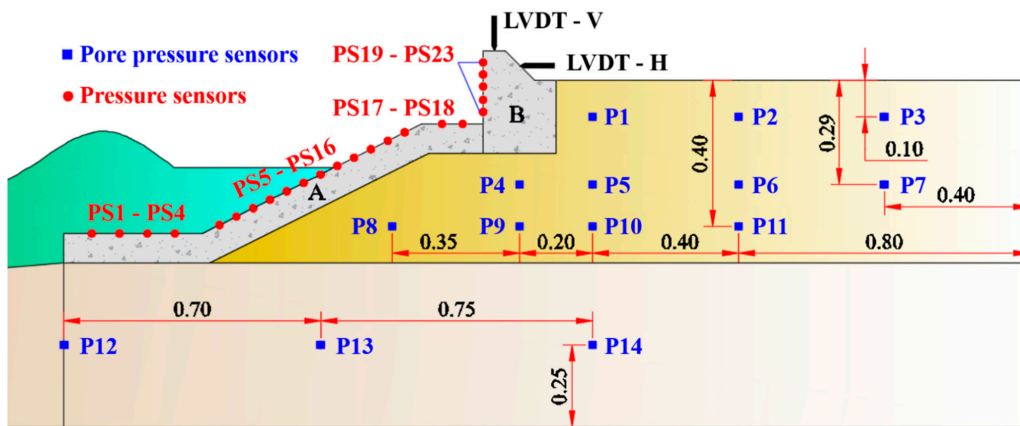


Figure 2. Schematic map of the location of the 14 pore pressure sensors, 23 pressure sensors and 2 displacement sensors (LVDT (Linear Variable Differential Transformer)) in the physical model (unit: m).

In order to relatively precisely control the accuracy of the dry density of the reclaimed coral sand foundation, the physical model is built layer by layer, with the help of a plate-type vibrator, making sure the dry density of each layer reaches its expected value. In this process, these pore pressure sensors are installed to their preset positions. The completed physical model with and without armor blocks is shown in Figures 3 and 4. It is worthy of notice that the wave flume is divided into two parts in its width direction at the section where the physical model is constructed. As a result, the water in front of, and behind, the physical model is naturally connected together in wave flume. Therefore, the overtopped water can return back to the water domain quickly in the wave flume without any loss.



Figure 3. A real view of the completed physical model without accropodes or rubble in front of the revetment breakwater.

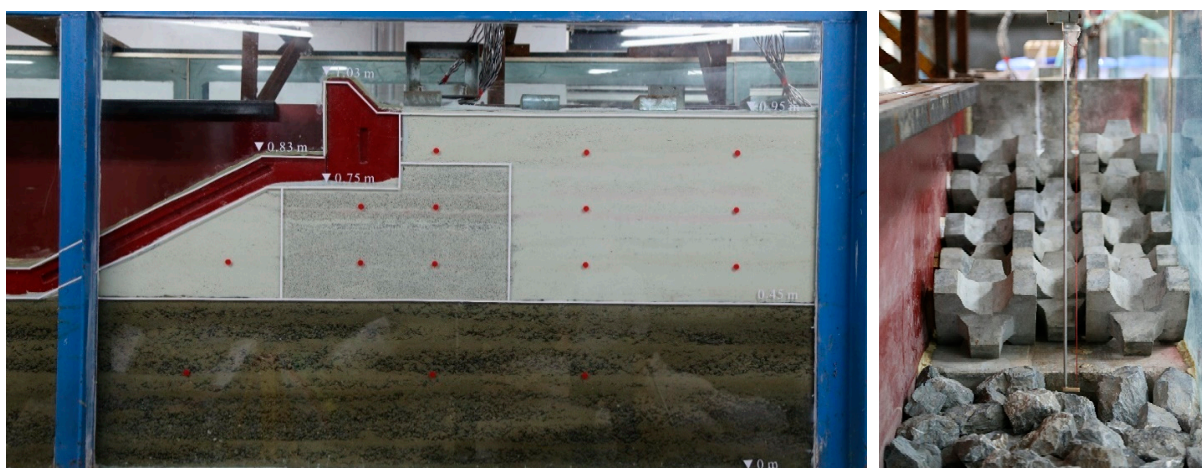


Figure 4. A real view of the completed physical model with accropodes and rubble in front of revetment breakwater.

The reclaimed coral sand foundation of the artificial islands in the South China Sea may be in a loose state due to the adverse influence of the construction technology or the limited time for the construction. In addition, it is widely recognized that the breakwater will be at great risk if its foundation is loose. Therefore, the main purpose of this study is to experimentally evaluate the stability of the revetment breakwater built on reclaimed loose coral sand foundation in the South China Sea under the long-term impact of extreme regular wave. In addition, it is also hoped to explore the effect of some factors, such as dry densities of the reclaimed coral sand foundation, armor blocks, tidal level and the wave period on the stability of the revetment breakwater. Accordingly, two dry densities of the reclaimed coral sand foundation, two water depths, two wave periods are set in the tests, and armor blocks are used in Test 4, Test5 and Test6, as illustrated in Table 3.

Table 3. Test conditions considering the wave parameters and the wave energy dissipation measure.

Test No.	Dry Density * (kg/m ³)	SWL (m)	Wave Height (m)	Wave Period (s)	Armor Blocks	Time (h)
1	1320	0.48	0.19	3.0	No	2
2	1320	0.71	0.30	2.2	No	2
3	1320	0.71	0.30	3.0	No	4
4	1320	0.71	0.30	3.0	Accropodes	2
5	1320	0.71	0.30	3.0	Rubbles	2
6	1320	0.71	0.30	3.0	Accropodes + Rubbles	2
7	1500	0.71	0.30	3.0	No	2

* Note: Dry density of the reclaimed coral calcareous sand foundation.

3. Results Analysis

A regular wave with a great wave height and a long wave period would bring great threat to the stability of a breakwater if there are no armor blocks used to dissipate wave energy in front of the breakwater and if there was an astronomical tide occurring at that time. Based on this recognition, Test 3 is taken as the typical test to analyze the dynamics and the stability of the revetment breakwater built on the loose reclaimed coral sand foundation in the South China Sea. Other tests will be used to explore the effect of water depth, wave period and armor blocks on the dynamics and stability of the revetment breakwater under the action of regular wave.

3.1. Wave Profiles

Wave profiles recorded in Test 3 are shown in Figure 5. As can be seen in Figure 5, the first wave reaches W1 at about 7 s and reaches W8 at 15 s. The waveform is relatively regular at W1–W6, which are far away from the revetment breakwater, while the waveform is irregular due to the effect of topography and the wave reflection at W7 and W8 near the revetment breakwater.

3.2. Displacement of Breakwater and Overtopping

Displacement is a direct criterion to assess the stability of revetment breakwater. The horizontal and vertical displacements of structure B recorded in Test 3 are shown in Figure 6. As illustrated in Figure 6, the horizontal displacement of structure B is very small and can be ignored. However, the vertical displacement of structure B increases rapidly in the first hour. After that, the increment of vertical displacement gradually decreases in the following three hours, and it basically reaches the final stable state at the end of test. The final settlement of structure B is about 6 mm. It can be observed that the revetment breakwater built on the loose reclaimed coral sand foundation in the South China Sea will have a settlement of 6 cm under the long-term impacting of waves according to the geometrical scale. In fact, this magnitude of displacement will not cause irreparable damage to the revetment breakwater. Therefore, the stability of the revetment breakwater can be basically guaranteed.

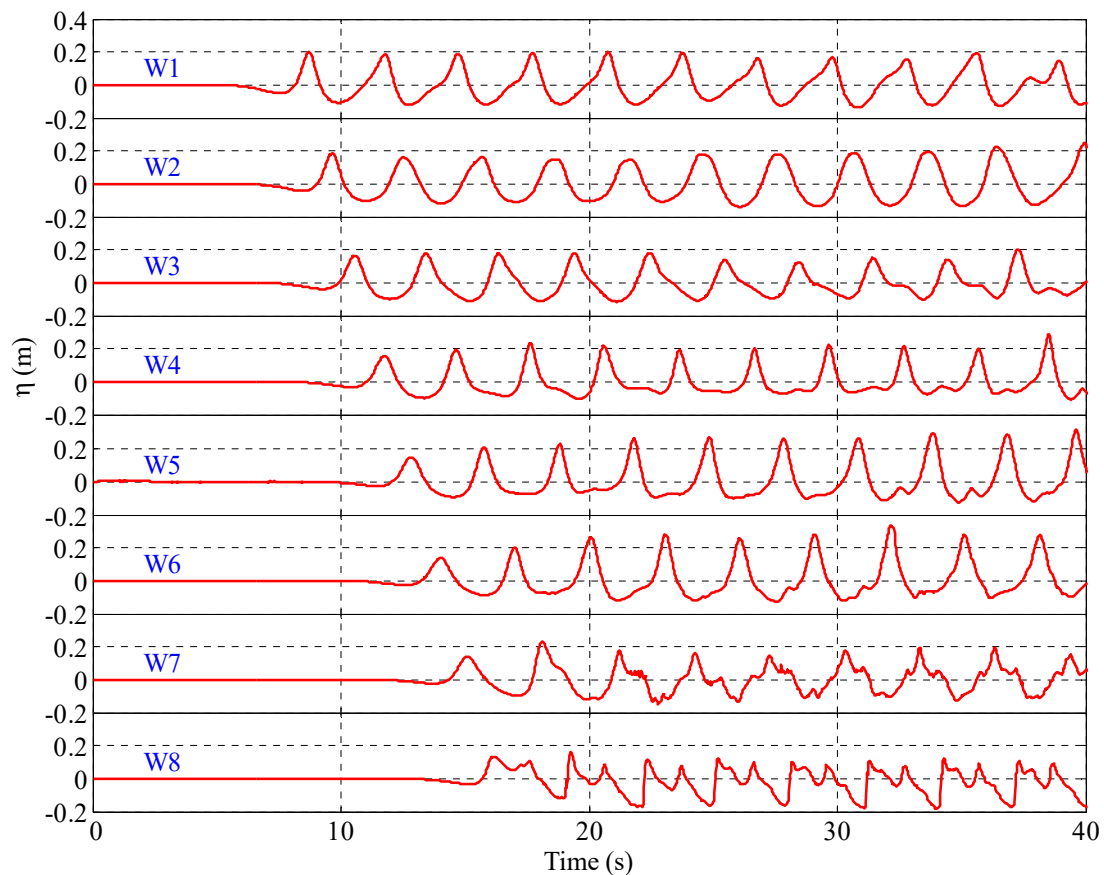


Figure 5. Wave profiles recorded in Test 3 ($d = 0.71$ m, $H = 0.3$ m, $T = 3.0$ s).

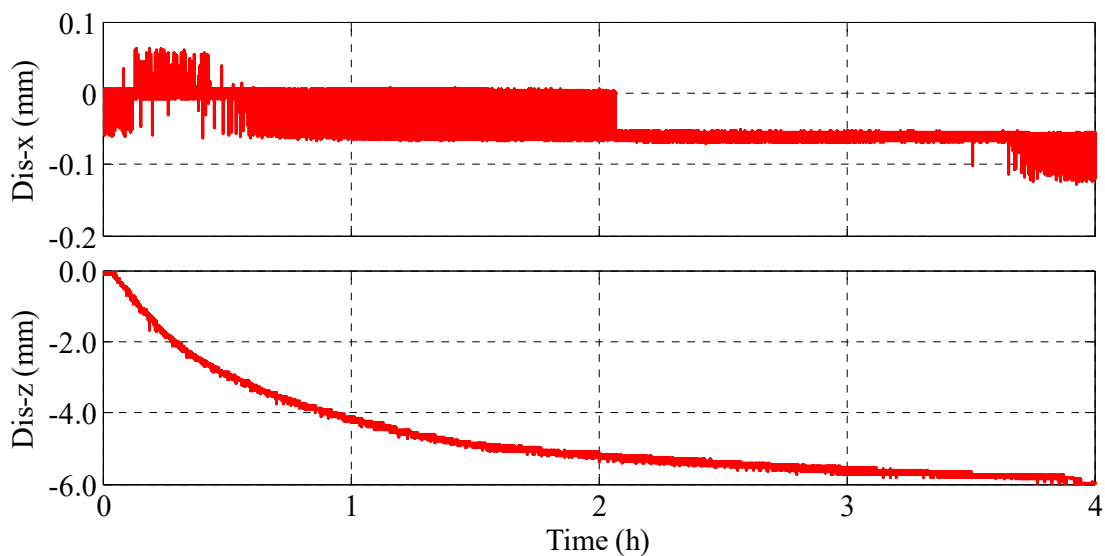


Figure 6. Time history of the horizontal and vertical displacement of structure B recorded in Test 3.

Overtopping has occurred in Test 3 as shown in Figure 7. The time history of the accumulative water volume of overtopping water recorded in Test 3 is shown in Figure 8. As can be seen in Figure 8, the accumulative volume of the overtopping water in 4 h is about 1.45 m^3 per sectional meter. Suppose that the width of the artificial island is 1 km, and the overtopping water can be converted into the capacity of rainfall. Taking the geometric scale of the physical model into consideration, the resulting rainfall is about 290 mm/d, which belongs to the level of heavy storms. It is worth noting that once the large volume of

seawater passes over the revetment breakwater, it cannot be discharged quickly back to sea due to the blocking of structure B. This seawater would be accumulated on the surface of the reclaimed land. It will return to the sea slowly through the underground seepage and drainage system. As a result, the overtopped sea water will cause some fatal ecological disasters, such as the death of vegetation behind the revetment breakwater and pollution of the desalinated underground water. The results of this physical model test suggest that the revetment breakwater has a poor resistance to overtopping under the impacting of extreme storm.



Figure 7. Revetment breakwater is being impacted by regular wave and water overtopping is occurring, observed in Test 3.

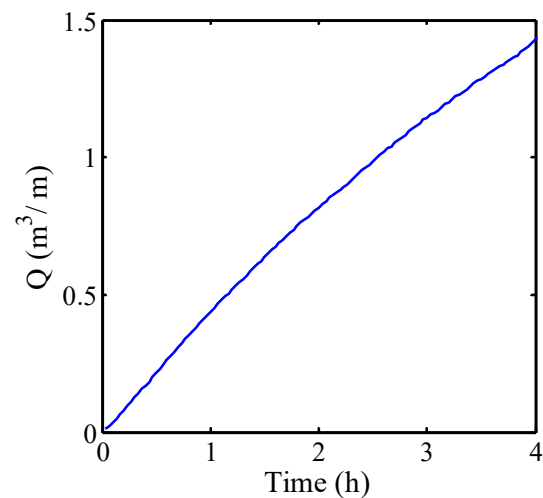


Figure 8. Time history of the accumulative volume of overtopping water recorded in Test 3.

3.3. Impact Pressure on the Revetment Breakwater

Safety and stability of the revetment breakwater are directly affected by the wave impact pressure. The results recorded at four typical locations are selected as the representative to analyze the impact pressure induced by the regular wave on structure A and B. The time history of the wave-induced impact recorded in Test 3 is shown in Figure 9. It can be found in Figure 9 that the impact pressure on the revetment breakwater is periodic. In addition, the impact pressure has two peaks in one period as marked in Figure 9. It is indicated that the incident wave is reflected by the revetment breakwater. Linear superposition of the wave impact induced by the incident wave and the reflected wave occurs in front of the revetment breakwater, resulting in the wave impact on the breakwater showing an “M” shape at the crests. This phenomenon has the typical characteristics of an impact force. The value of the wave impact recorded at PS20 is the largest one among the four typical positions. One conclusion can be made that the wave impact on structure B is much greater than that on structure A.

Distribution of the maximum wave impact on the surface of the revetment breakwater under regular wave loading in Test 3 is shown in Figure 10. It can be seen in Figure 10 that the maximum impact force is recorded at the top of structure B, and the value is about 17.27 kPa. From the above analysis, it is known that structure B acts as a vertical reflection boundary. Therefore, structure B is subjected to a great impact under regular wave action.

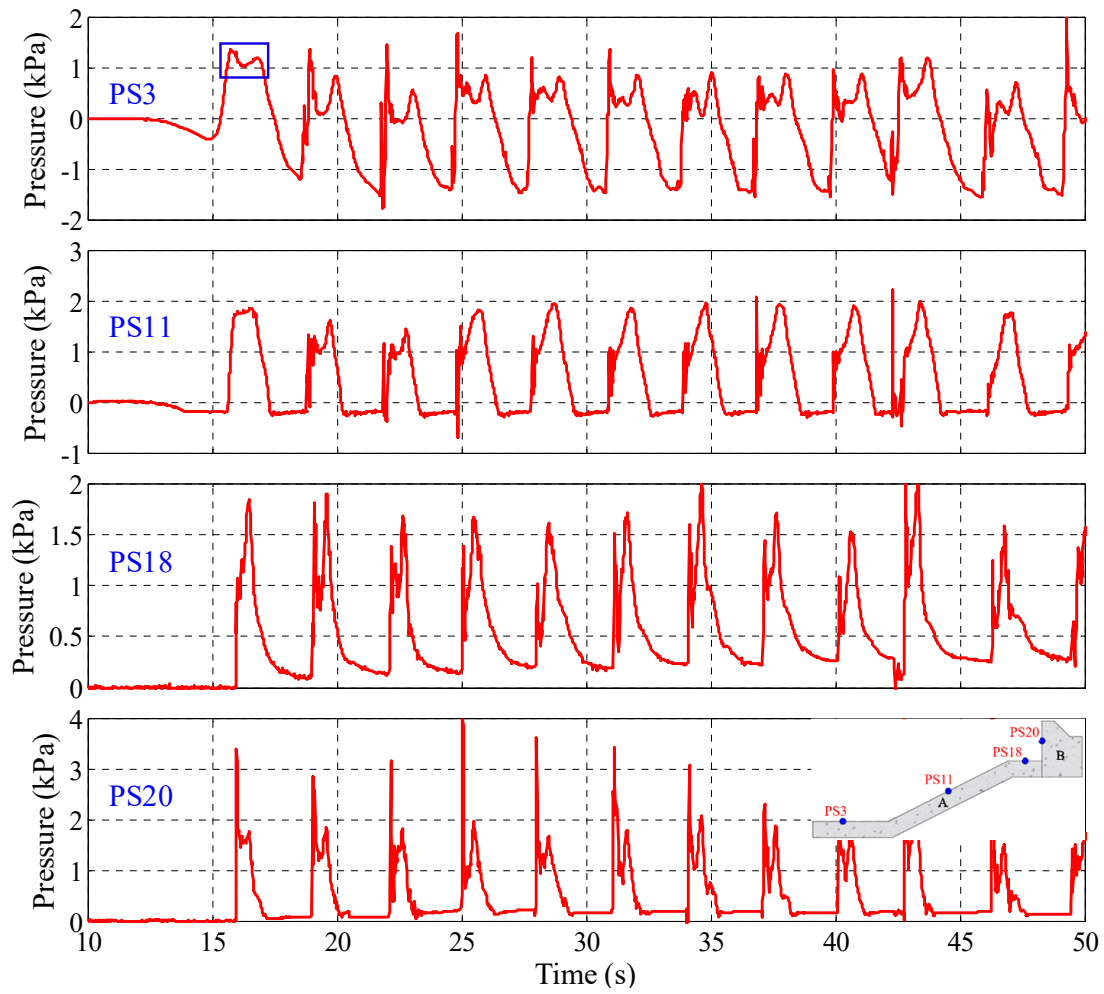


Figure 9. Time history of the wave impact recorded in Test 3 at the four typical positions (hydrostatic pressure is excluded).

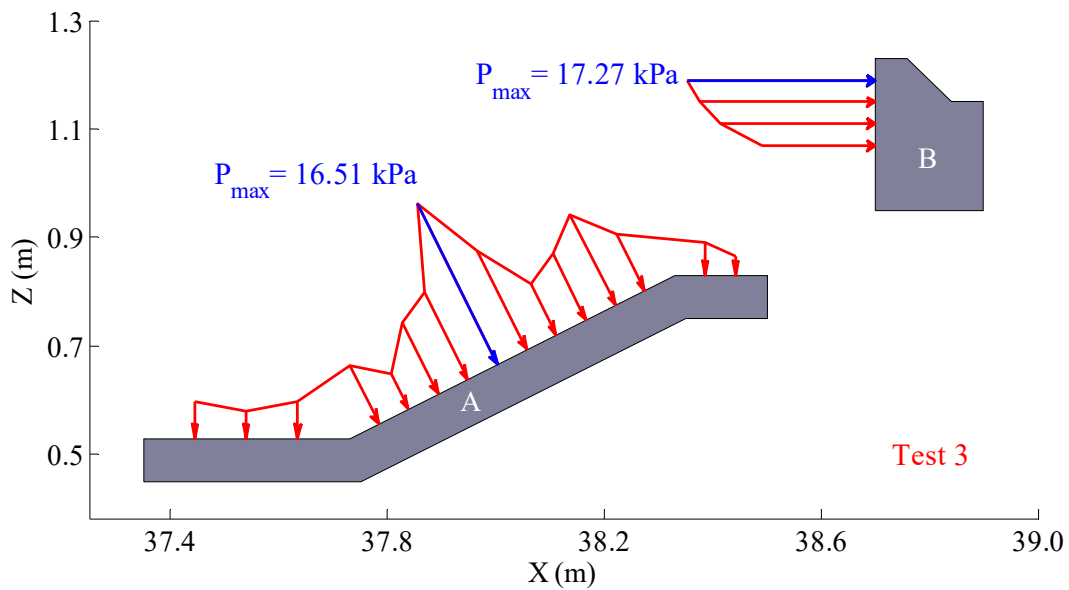


Figure 10. Distribution of the maximum wave impact on the surface of the revetment breakwater under regular wave action in Test 3.

The time history of the impact force on structure A and B recorded in Test 3 is shown in Figure 11. As can be seen in Figure 11, the maximum value of impact force on structure A is about 0.45 kN per sectional meter in the horizontal direction and 0.65 kN per sectional meter in the vertical direction. The maximum value of impact force on structure B is about 1.8 kN per sectional meter in the horizontal direction. It is found that the wave impact force on structure B is much greater than that on structure A, which is consistent with the analysis above. Based on observation in this test, no failure has been observed. The breakwater finally reaches a stable state after a certain amount of settlement, as shown in Figure 6. It can be deduced that the revetment breakwater can basically keep stable under the impact of this regular wave due to the strong support supplied by the passive pressure of the reclaimed coral sand foundation behind the caisson wall.

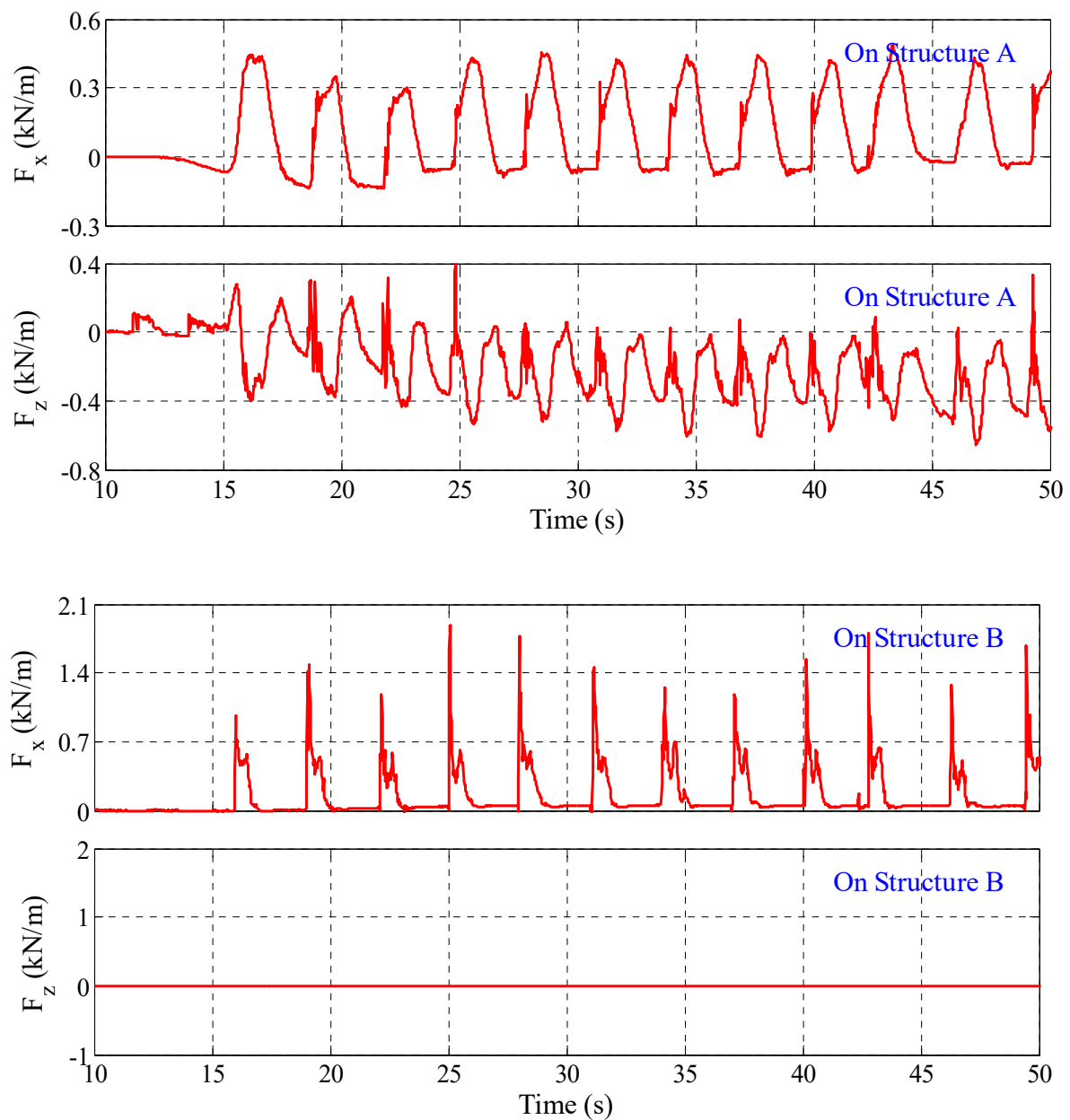


Figure 11. Time history of the impact force on structure A and B applied by regular wave in Test 3.

3.4. Pore Pressure in the Reclaimed Coral Sand Foundation

The dynamic response of pore pressure directly affects the strength of reclaimed coral sand foundation below and behind the revetment breakwater. Excessive pore pressure would lead to the reduction in effective stress, resulting in the softening or liquefaction of sand foundation. In this section, the physical mechanism of the behavior of the reclaimed coral calcareous will be further revealed by analyzing the dynamic response of pore pressure. The time history of the dynamic response of pore pressure recorded by the 13 pore pressure sensors in Test 3 is shown in Figure 12.

As can be seen in Figure 12, pore pressure in the reclaimed coral sand foundation overall gradually accumulates under the cyclic wave loading and reaches their maximum value in about 10 cycles of wave loading. The maximum increment of pore pressure is 1.5 kPa. Does the accumulation of pore pressure cause softening or liquefaction in the reclaimed coral sand foundation or not?

Firstly, as shown in Figure 12, the accumulation of pore pressure only occurs in the first 10 cycles of wave impact. Secondly, the revetment breakwater finally reaches a stable state and there is no obvious failure in Test 3, according to the previous analysis. It can be concluded that no softening or liquefaction occurs in the reclaimed coral sand foundation. The physical mechanism of interaction of waves, breakwater and loose reclaimed coral sand foundation can be explained.

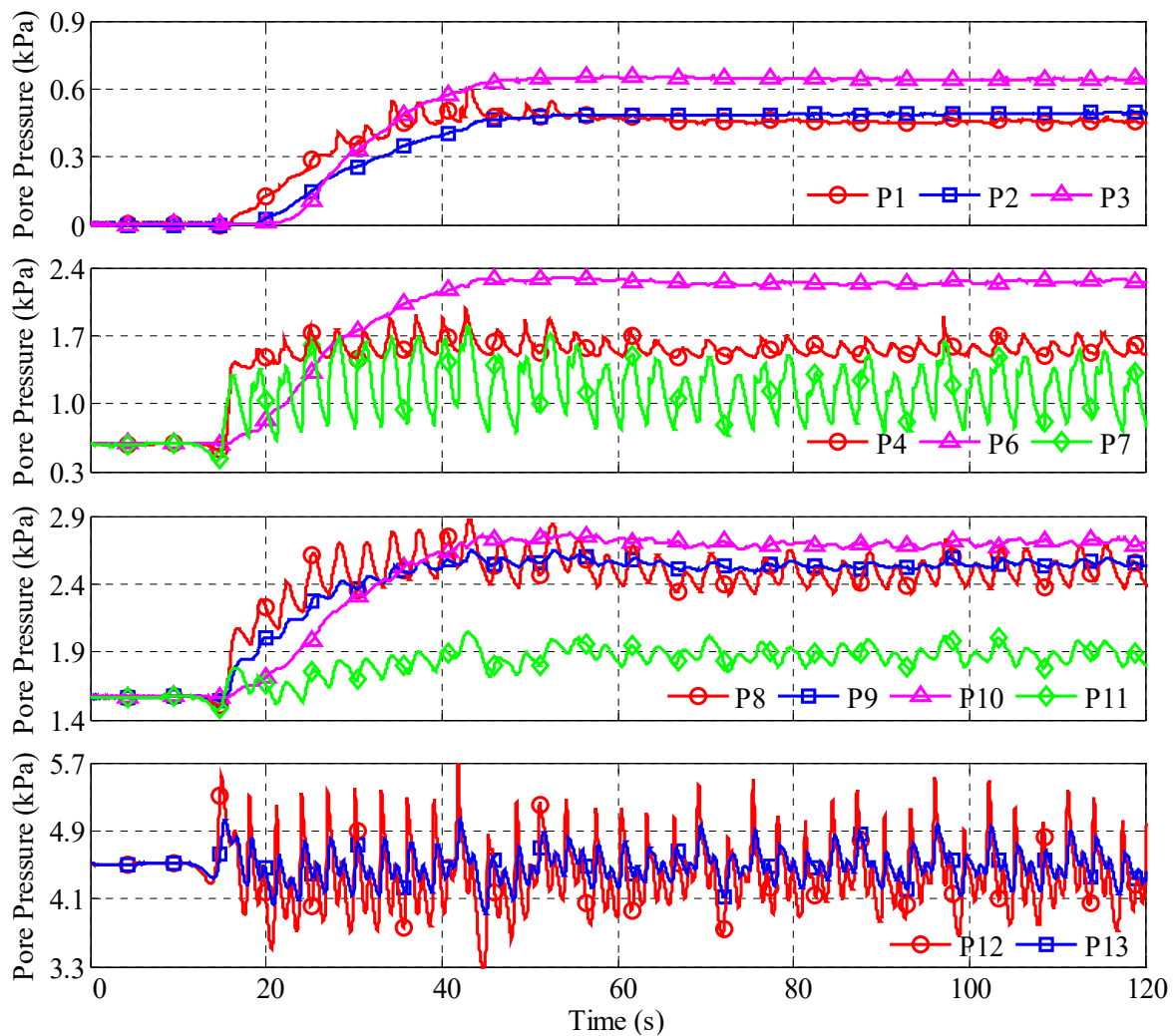


Figure 12. Time history of the wave-induced pore pressure in the reclaimed coral sand foundation in Test 3 (in the first 2 min).

Soil particles in the reclaimed loose coral sand foundation rearrange towards a dense state under the cyclic wave impacting. As a result, structure B settles under the influence of gravity, and excessive pore pressure is generated in the reclaimed coral sand foundation. Finally, rearrangement of the soil particles is completely finished, and the loose reclaimed coral sand foundation becomes dense. The system composed of the revetment breakwater and the reclaimed coral sand foundation reach a new equilibrium.

The momentary and residual pore pressure recorded at P1, P4, P8 and P12 in Test 3 are shown in Figure 13. As illustrated in Figure 13, the residual pore pressure in the reclaimed sand foundation increases significantly at first, and then oscillates within a certain range. The oscillation period of the residual pore pressure is about 100 s, which is 33 times of the wave period. The oscillation of the residual pore pressure may be caused by the gradual accumulation of reflected wave energy in the wave flume.

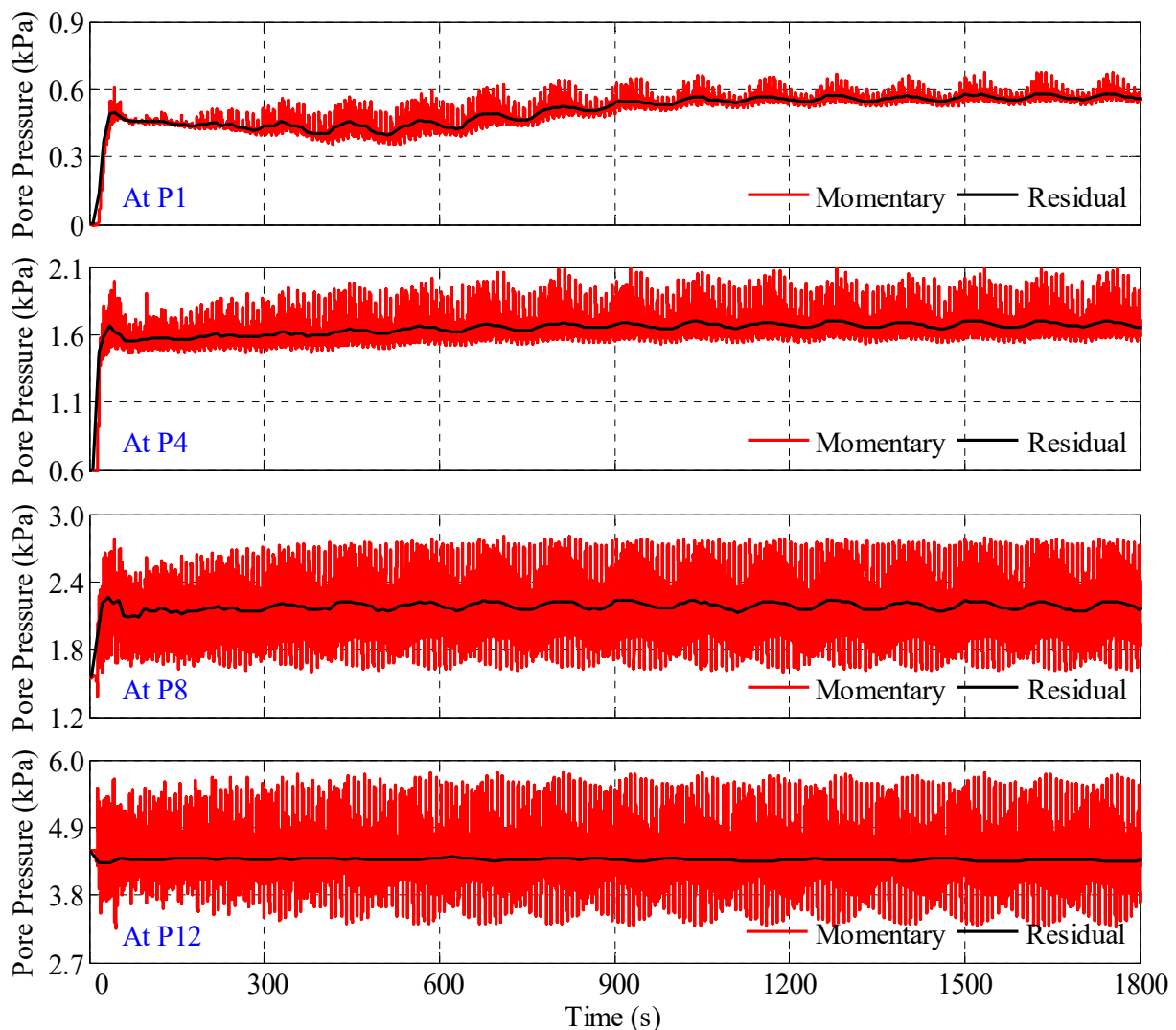


Figure 13. Momentary and residual pore pressure recorded at P1, P4, P8 and P12 in Test 3 (in the first 30 min).

4. Analysis of Affecting Factors

Previous studies have shown that the tidal level, wave period, and the armor blocks would have some effects on the stability of a breakwater. This section is aimed to explore the effects of these factors, respectively, on the stability of the revetment breakwater through comparative study.

4.1. Effect of Tidal Level

The tidal level is changed periodically due to the astronomic conditions during the designed service period of the revetment breakwater. There is a direct relationship between the wave impact on the revetment breakwater and the tidal level. In this section, the effect of tidal level will be explored by comparing the test results recorded in Test 1 ($d = 0.48$ m) and in Test 3 ($d = 0.71$ m). Distribution of the maximum wave impact on structure A and structure B recorded in Test 1 is shown in Figure 14. Comparison of wave impact force on structure A and structure B measured in Test 1 and Test 3 is shown in Figure 15. Comparison of pore pressure recorded at P1, P4, P8 and P12 between Test 1 and Test 3 is shown in Figure 16. Obviously, the wave impact on the revetment breakwater and wave-induced pore pressure in the reclaimed coral sand foundation recorded in Test 3 are much greater than that recorded in Test 1. It can be concluded that the wave will bring less threat to the stability of the revetment breakwater at low tide level.

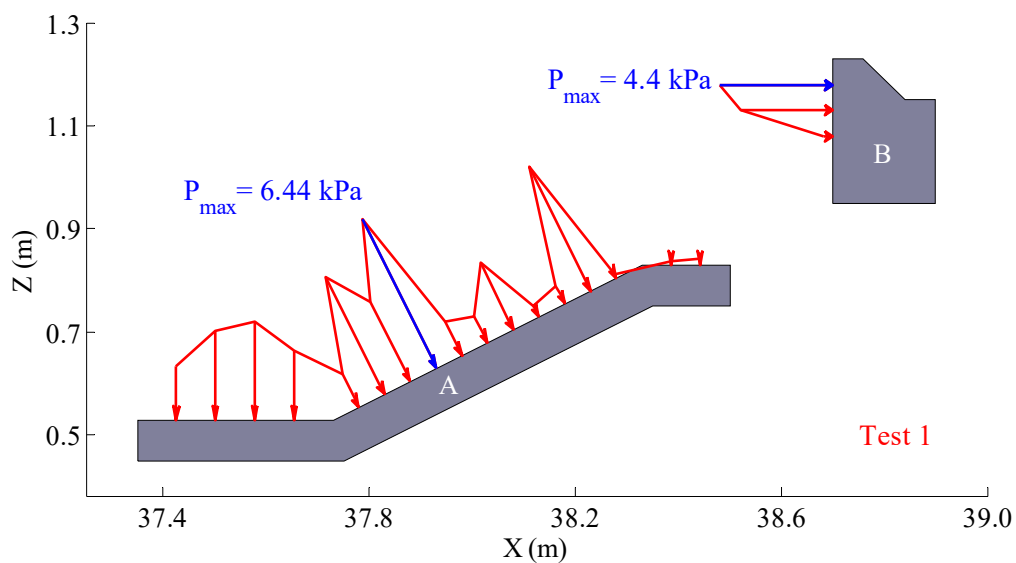


Figure 14. Distribution of the maximum wave impact on the surface of the revetment breakwater under regular wave loading in Test 1.

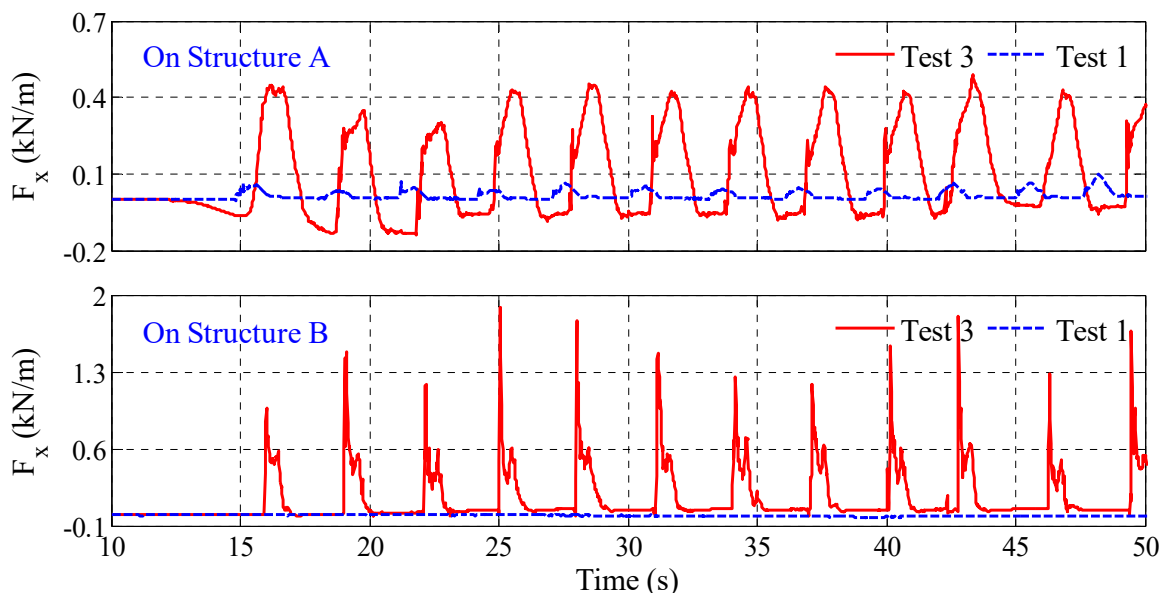


Figure 15. Comparison of wave impact force on structure A and B measured in Test 3 ($d = 0.71$ m) and Test 1 ($d = 0.48$ m).

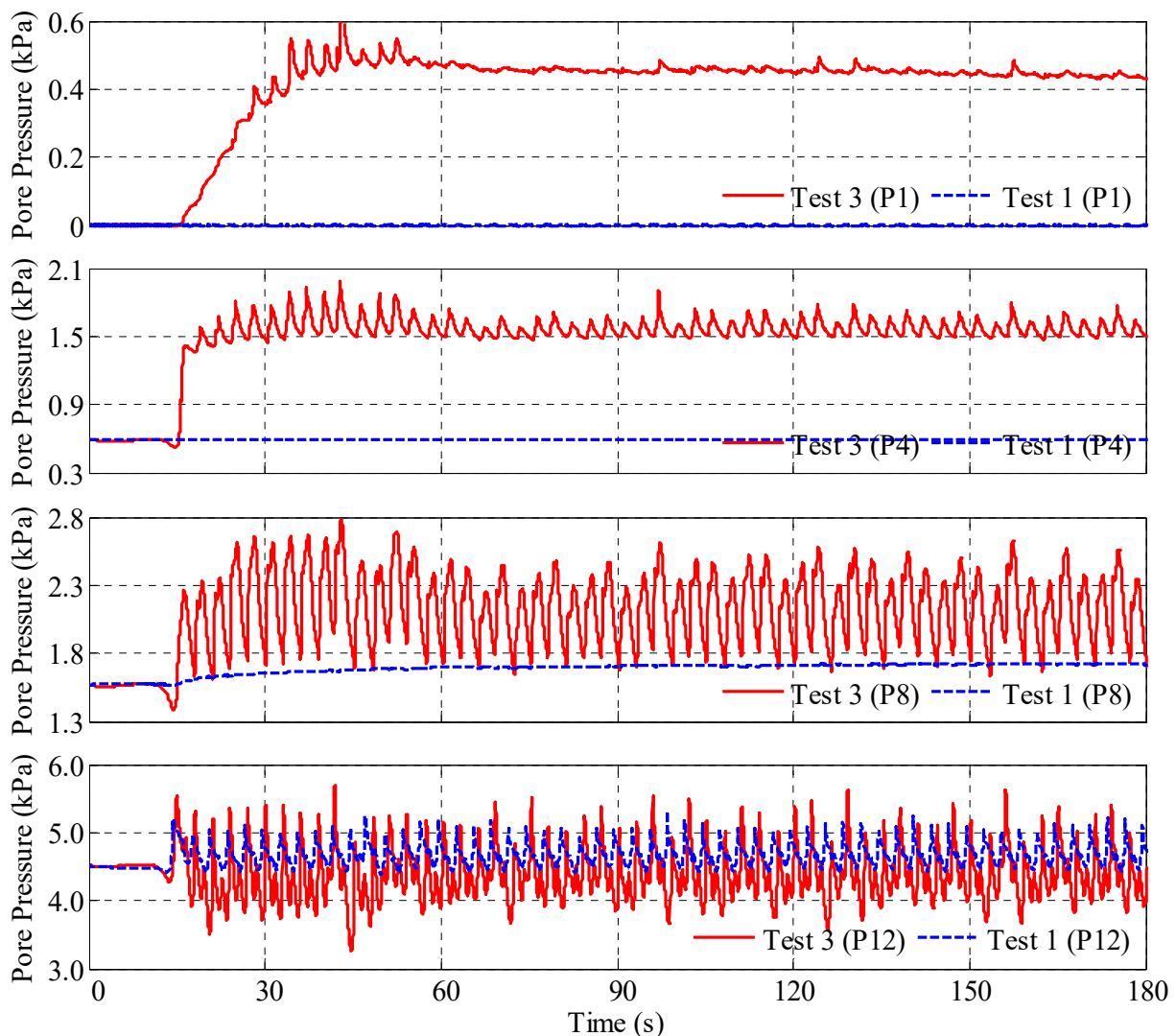


Figure 16. Comparison of pore pressure recorded at P1, P4, P8 and P12 between Test 3 ($d = 0.71$ m) and Test 1 ($d = 0.48$ m).

4.2. Effect of Wave Period

The effect of wave period can be studied by comparing the test results recorded in Test 2 ($T = 2.0$ s) and in Test 3 ($T = 3.0$ s). Distribution of the maximum wave impact on the surface of the revetment breakwater under regular wave loading in Test 2 is shown in Figure 17. It can be seen in Figures 10 and 17 that the distribution and values of the maximum wave impact on revetment breakwater recorded in Test 2 and Test 3 are basically the same. Comparison of wave impact force on structure A and B measured in Test 2 and Test 3 is shown in Figure 18. Comparison of pore pressure recorded at P1, P4, P8 and P12 between Test 2 and Test 3 is shown in Figure 19. It is found that the wave-induced impact force on the revetment breakwater and the pore pressure in the reclaimed sand foundation recorded in Test 2 are smaller than that in Test 3. Table 4 demonstrates that the vertical displacement of structure B is 3 mm and the overtopping is 169.46 kg per sectional meter in Test 2, which are about 1/2 of that in Test 3. The above results indicate that the regular wave with a longer period will cause greater adverse effects on the stability of breakwater.

Table 4. Displacement of structure B and overtopping in Test 1 to Test 6.

Test No.	Test 1	Test 2	Test 3	Test 4	Test 5	Test 6	Test 7
Displacement-x (mm)	0.1	0.1	0.1	0.1	0.1	0.1	0.5
Displacement-z (mm)	-0.2	-3.0	-6.0	-0.4	-1.1	-0.3	0.3
Overtopping (m ³ /(m·h))	0	0.1695	0.3578	0.9136	0.9921	0.8990	0.3219

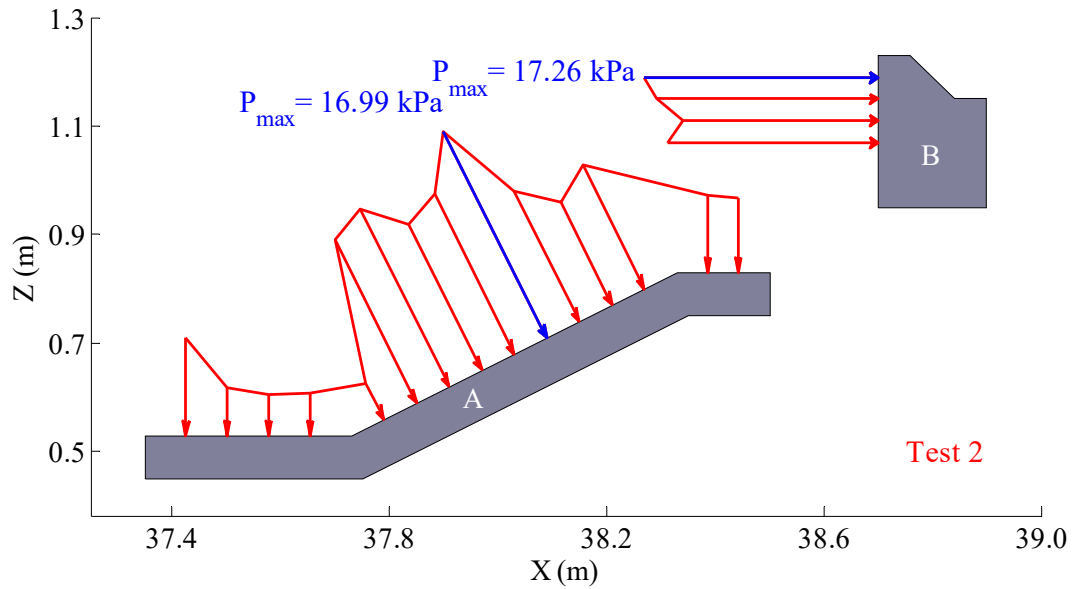


Figure 17. Distribution of the maximum wave impact on the surface of the revetment breakwater under regular wave loading in Test 2.

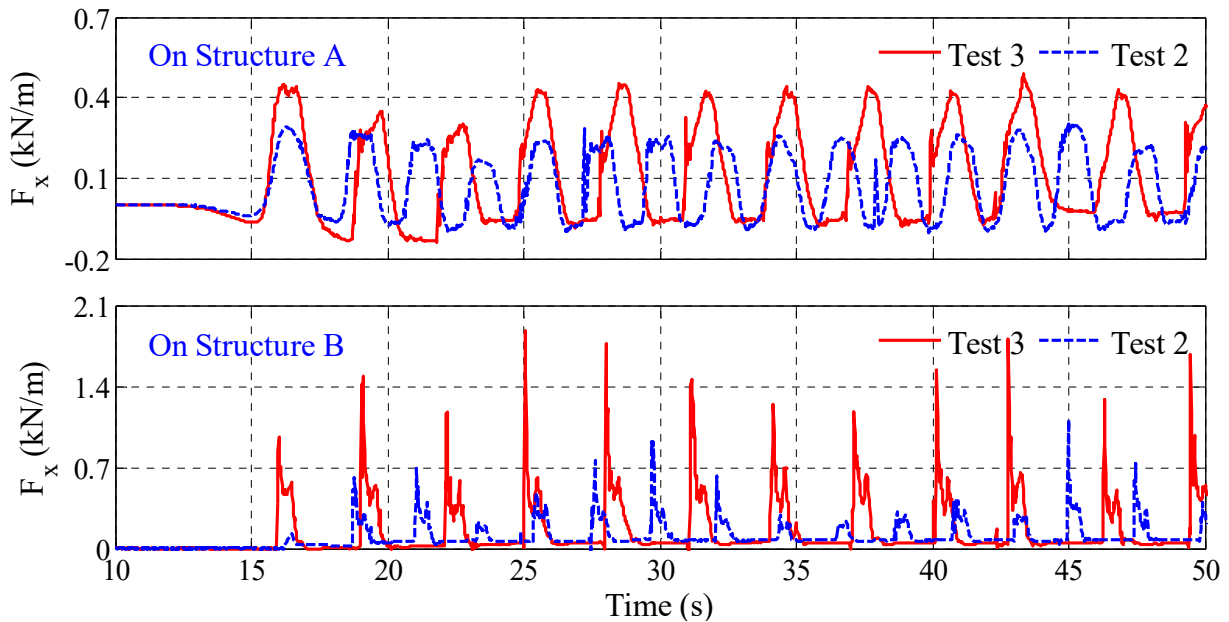


Figure 18. Comparison of wave impact force on structure A and B measured in Test 3 ($T = 3.0$ s) and Test 2 ($T = 2.2$ s).

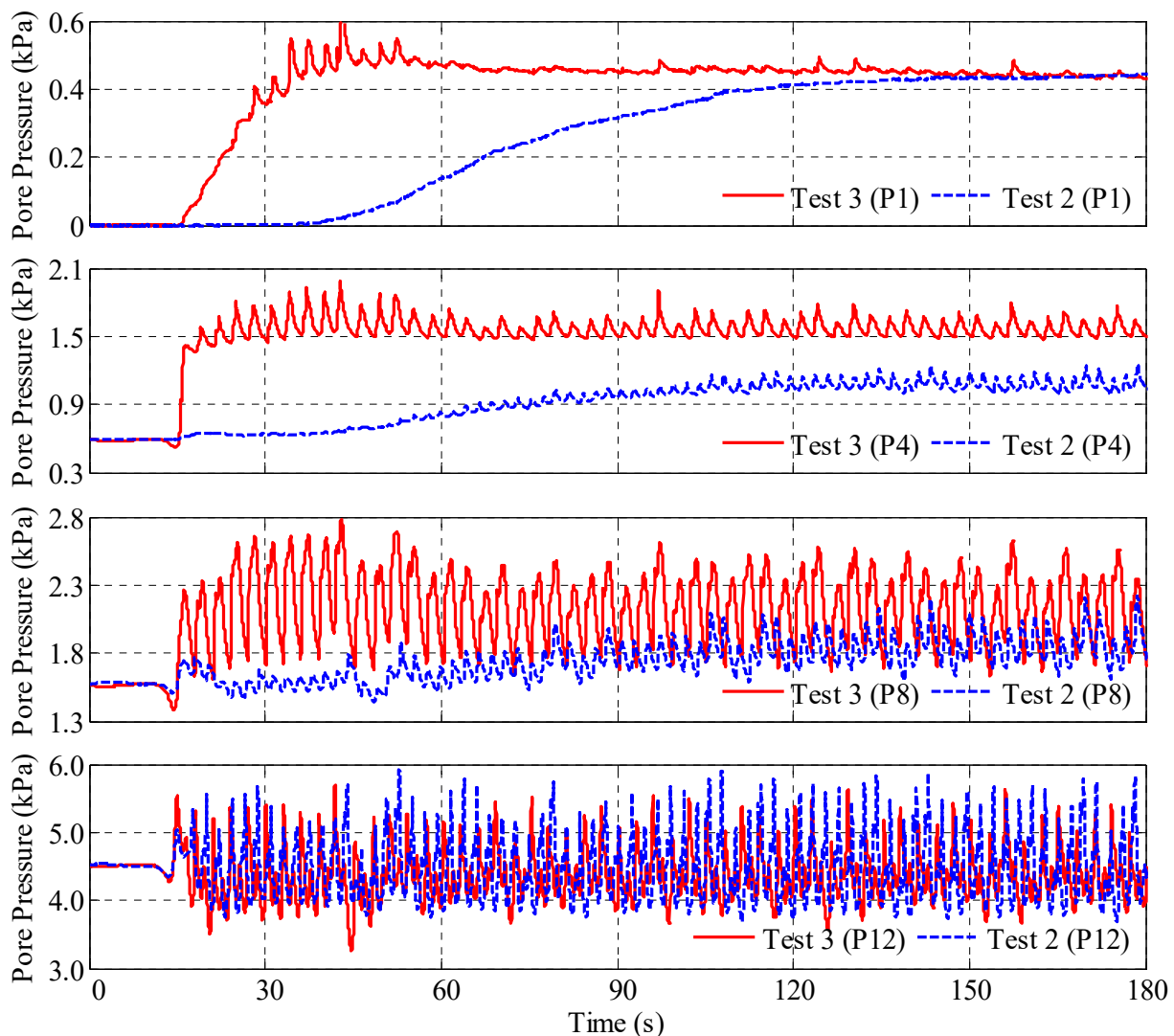


Figure 19. Comparison of pore pressure recorded at P1, P4, P8 and P12 between Test 3 ($T = 3.0$ s) and Test 2 ($T = 2.2$ s).

4.3. Effect of Armor Blocks

Previous researchers have shown that armor blocks such as accropodes can effectively reduce the wave-induced impact force on breakwater [41]. This section is aimed to explore the effect of the armor blocks on enhancing the stability of the revetment breakwater by comparative study. Accropodes are laid on the revetment breakwater in Test 4, rubbles are laid in Test 5, accropodes and rubbles are jointly adopted in Test 6. Distribution of the maximum wave impact on the surface of the revetment breakwater under the wave loading in Test 4, Test 5 and Test 6 is shown in Figure 20. Comparison of the wave impact force on structure A and B measured in Test 3, Test 4, Test 5 and Test 6 is shown in Figure 21. It is found that the wave impact on the revetment breakwater is obviously small in Test 4 and in Test 6, especially for the wave impact on structure B. The wave-induced impact on the breakwater recorded in Test 3 and Test 5 is basically the same. It is indicated that the accropodes can help to dissipate the wave energy and protect the revetment breakwater; especially for structure B, the protection effect is more significant. Meanwhile, the rubble plays little role in dissipating the wave energy.

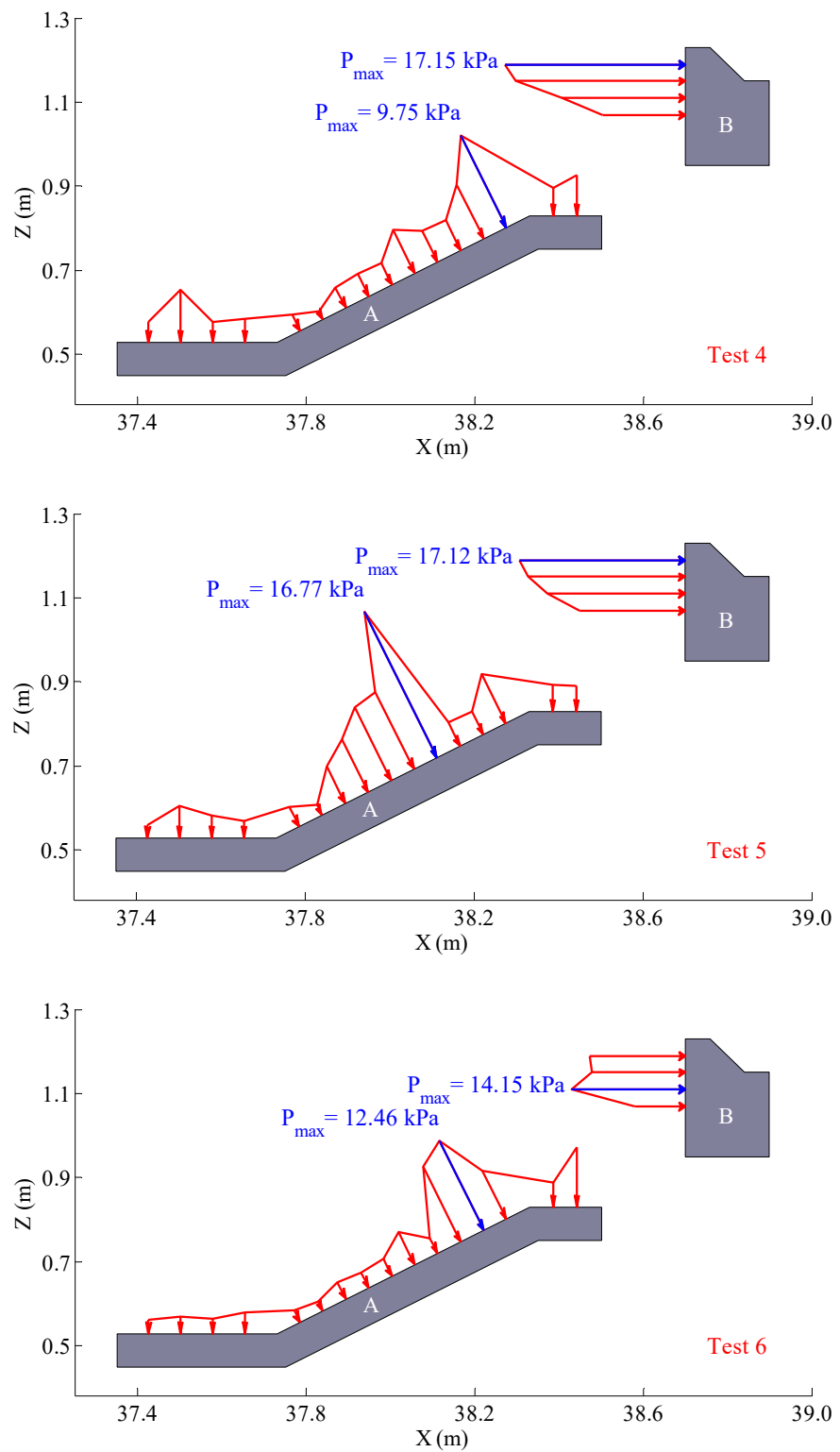


Figure 20. Distribution of the maximum wave impact on the surface of the revetment breakwater under regular wave loading in Test 4 (accropodes), Test 5 (rubble) and Test 6 (accropodes and rubble).

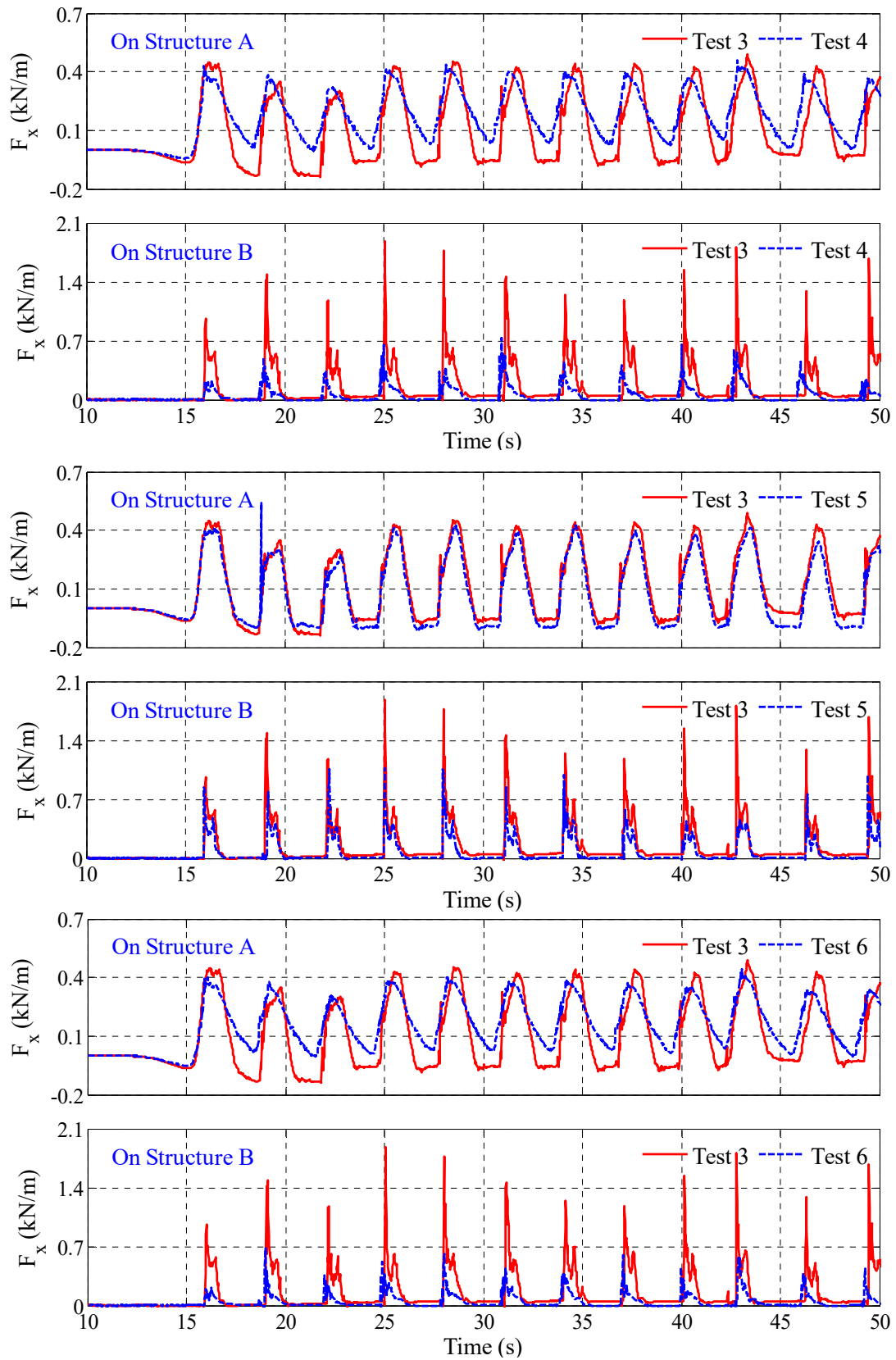


Figure 21. Comparison of the wave impact force on structure A and B measured in Test 3 (no armor block), Test 4 (accropodes), Test 5 (rubble) and Test 6 (accropodes and rubble).

Comparison of the pore pressure recorded at P1, P4, P8 and P12 among Test 3, Test 4, Test 5 and Test 6 is shown in Figure 22. It can be seen in Figure 22 that the pore pressure recorded in Test 6 is the smallest. Table 4 also shows similar phenomenon that the displacement of the revetment breakwater and the overtopping water measured in Test 6 are the smallest. Conclusions can be made that the accropodes will help to maintain the stability of revetment breakwater under wave impact. The protection effect for breakwater is more significant when accropodes and rubble is jointly adopted to dissipate the energy of waves.

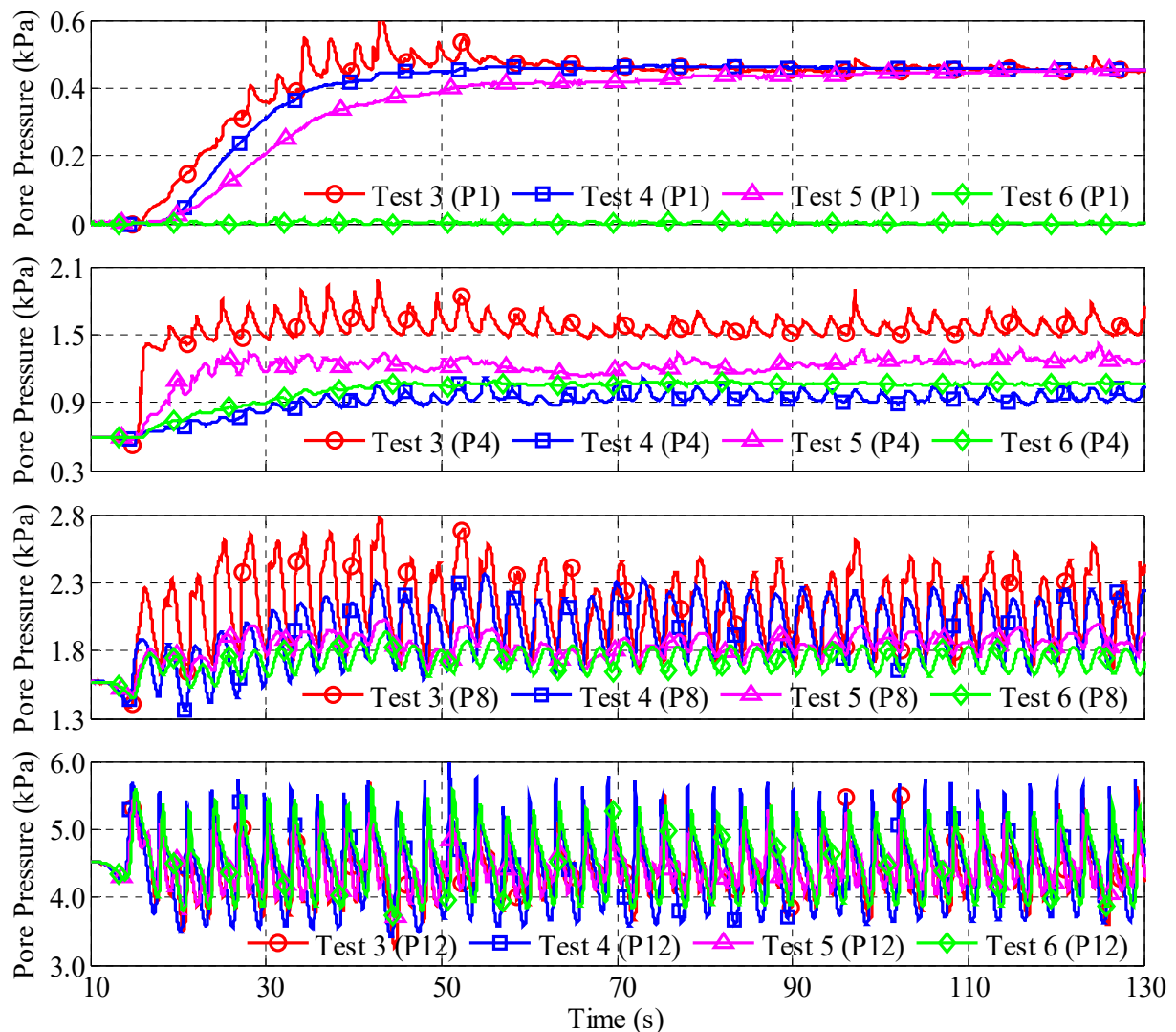


Figure 22. Comparison of the pore pressure recorded at P1, P4, P8 and P12 among Test 3 (no armor block), Test 4 (accropodes), Test 5 (rubble) and Test 6 (accropodes and rubble).

4.4. Effect of Foundation Density

It is widely recognized that dry density of the reclaimed coral sand foundation has an important effect on the settlement of breakwater and the dynamic response of pore pressure. In this section, the effect of the dry density of the reclaimed coral sand foundation on the stability of revetment breakwater is studied by comparing the test results recorded in Test 3 and Test 7. The dry density of the reclaimed coral sand foundation is 1500 kg/m^3 in Test 7, and 1320 kg/m^3 in Test 3. Comparison of the pore pressure recorded in Test 3 and Test 7 is shown in Figure 23. It is found that the amplitude and oscillation amplitude of pore pressure at P4 and P8 recorded in Test 3 are both greater than that in Test 7. This

phenomenon indicates that pore pressure is more easily accumulated in relatively loose sand foundation. Combining the test results listed in Table 4, the settlement of structure B measured in Test 7 is only 3 mm, which is much smaller than that measured in Test 3. A conclusion can be made that the revetment breakwater is more stable if the dry density of its foundation is relatively dense.

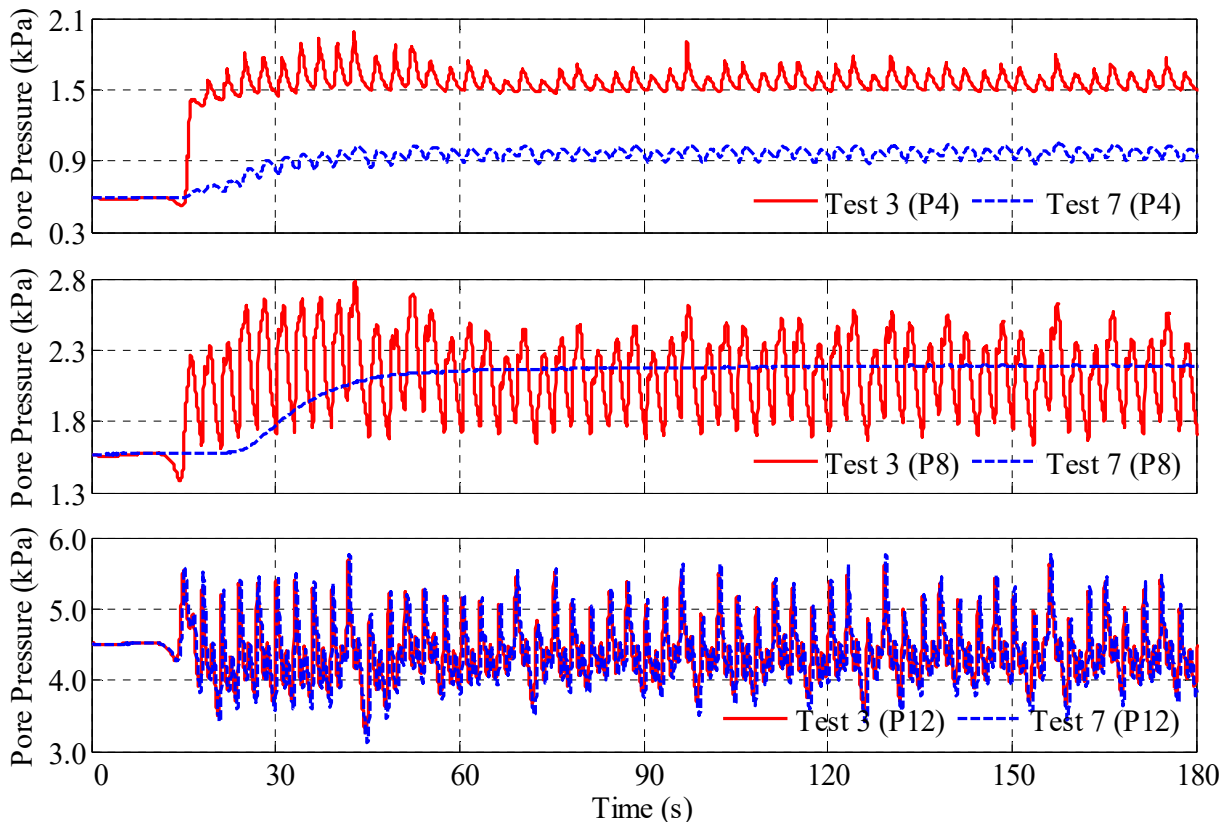


Figure 23. Comparison of pore pressure recorded at P4, P8 and P12 between Test 3 ($\rho_d = 1320 \text{ kg/m}^3$) and Test 7 ($\rho_d = 1500 \text{ kg/m}^3$).

5. Conclusions

In this study, taking the reclamation engineering in the South China Sea as the engineering background, a series of large-scale physical model tests are conducted out to study the stability of revetment breakwater built on the reclaimed coral sand foundation in South China Sea under the impact of regular wave. Based on the experimental results, the following conclusions are drawn:

1. The maximum final settlement of the revetment breakwater is only 6 mm if it is built on loose coral sand foundation. This magnitude of displacement will not cause irreparable damage to the revetment breakwater.
2. Pore pressure in the coral sand foundation basically could only accumulate in the first 10 cycles of wave impacting. The maximum excess pore pressure in the loose reclaimed coral sand foundation is only 1.5 kPa. No softening or liquefaction occurs in the reclaimed coral sand foundation. This is a favorable condition for the stability of the revetment breakwater.
3. The accumulative volume of the overtopping water in 4 h is about 1.45 m^3 per sectional meter under the extreme wave impacting. This overtopped sea water would cause fatal ecological disasters to the artificial islands in the South China Sea.
4. The wave will bring greater threat to the stability of the revetment breakwater if the tide level is higher, the foundation is looser, and the wave period is longer. Accropodes

could significantly enhance the stability of the revetment breakwater under severe wave impacting.

Author Contributions: Conceptualization, J.Y.; formal analysis, K.H. and J.Y.; funding acquisition, J.Y.; investigation, K.H. and J.Y.; methodology, K.H. and J.Y.; project administration, J.Y.; supervision, J.Y.; visualization, K.H.; writing—original draft, K.H.; writing—review and editing, J.Y. Both authors have read and agreed to the published version of the manuscript.

Funding: This work is grateful for the funding support from National Natural Science Foundation of China, Grant No. 51879257, as well as the funding support from “Strategic Priority Research Program of the Chinese Academy of Sciences”, Grant No. XDA13010202.

Institutional Review Board Statement: Not applicable.

Informed Consent Statement: Not applicable.

Data Availability Statement: Some data that support the findings of this study are available from the corresponding author upon reasonable request. Meanwhile, some data generated or used during the study are proprietary or confidential in nature and may only be provided with restrictions.

Conflicts of Interest: The authors declare no conflict of interest.

References

1. Wu, J.X. *Collapse Analysis of Lianyungang West Breakwater*; National Library Collection: Beijing, China, 1957. (In Chinese)
2. Gu, X.Y. Review and prospects of marine engineering geology. *J. Eng. Geol.* **2000**, *8*, 40–45. (In Chinese)
3. Zen, K.; Umehara, Y.; Finn, W.D.L. A case study of the wave-induced liquefaction of sand layers under the damaged breakwater. In Proceedings of the Third Canadian Conference on Marine Geotechnical engineering, St. John’s, NL, Canada, 18 July 1986.
4. Medina, L.E.; Allsop, N.W.H.; Dimakopoulos, A.; Bruce, T. Conjectures on the Failure of the OWC Breakwater at Mutriku. In Proceedings of the Coastal Structures and Solutions to Coastal Disasters Joint Conference, Boston, MA, USA, 9–11 September 2015.
5. Guan, F.C.; Xie, Q.H. Statistical characteristics of typhoons in the South China Sea. *Mar. Sci. Bull.* **1984**, *3*, 21–29. (In Chinese)
6. Mizutani, N.; Mostafa, A.M. Nonlinear wave-induced seabed instability around coastal structures. *Coast. Eng. J.* **1998**, *40*, 131–160. [[CrossRef](#)]
7. Liu, L.F.; Lin, P.; Chang, K.A.; Sakakiyama, T. Numerical modelling of wave interaction with porous structures. *J. Waterw. Port Coast. Ocean Eng.* **1999**, *125*, 322–330. [[CrossRef](#)]
8. Jeng, D.S.; Cha, D.F.; Lin, Y.S.; Hu, P.S. Wave-induced pore pressure around a composite breakwater. *Ocean Eng.* **2001**, *28*, 1413–1435. [[CrossRef](#)]
9. Tsai, C.P.; Chen, H.B.; Lee, F.C. Wave transformation over submerged permeable breakwater on porous bottom. *Ocean Eng.* **2006**, *33*, 1623–1643. [[CrossRef](#)]
10. Hur, D.S.; Kim, C.H.; Kim, D.S.; Yoon, J.S. Simulation of the nonlinear dynamic interactions between waves, a submerged breakwater and the seabed. *Ocean Eng.* **2008**, *35*, 511–522. [[CrossRef](#)]
11. Hanzawa, M.; Matsumoto, A.; Tanaka, H. Stability of wave-dissipating concrete blocks of detached breakwaters against tsunami. *Coast. Eng. Proc.* **2012**, *33*, 24. [[CrossRef](#)]
12. Sawada, Y.; Miyake, M. Numerical analysis on stability of caisson-type breakwaters under tsunami-induced seepage. *Transp. Infrastruct. Geotechnol.* **2015**, *2*, 120–138. [[CrossRef](#)]
13. Guler, H.G.; Arikawa, T.; Oei, T.; Yalciner, A.C. Performance of rubble mound breakwaters under tsunami attack, a case study: Haydarpasa Port, Istanbul, Turkey. *Coast. Eng.* **2015**, *104*, 43–53. [[CrossRef](#)]
14. Ye, J.H.; Jeng, D.S.; Wang, R.; Zhu, C.Q. Validation of a 2-D semi-coupled numerical model for fluid-structure-seabed interaction. *J. Fluids Struct.* **2013**, *42*, 333–357. [[CrossRef](#)]
15. Ye, J.H.; Jeng, D.S.; Wang, R.; Zhu, C.Q. A 3-D semi-coupled numerical model for fluid-structures-seabed-interaction (FSSI-CAS 3D): Model and verification. *J. Fluids Struct.* **2013**, *40*, 148–162. [[CrossRef](#)]
16. He, K.P.; Huang, T.K.; Ye, J.H. Stability analysis of a composite breakwater at Yantai port, China: An application of FSSI-CAS-2D. *Ocean Eng.* **2018**, *168*, 95–107. [[CrossRef](#)]
17. Johnson, R.R.; Mansard, E.P.; Ploeg, J. Effects of wave grouping on breakwater stability. In *Coastal Engineering*; ASCE: Reston, VA, USA, 1978; Volume 1978, pp. 2228–2243.
18. Yagci, O.; Kapdasli, S.; Cigizoglu, H.K. The stability of the antifer units used on breakwaters in case of irregular placement. *Ocean Eng.* **2004**, *31*, 1111–1127. [[CrossRef](#)]
19. Li, Y.; Lin, M. Regular and irregular wave impacts on floating body. *Ocean Eng.* **2012**, *42*, 93–101. [[CrossRef](#)]
20. Jensen, T.; Andersen, H.; Grønbech, J. Breakwater stability under regular and irregular wave attack. In *Coastal Engineering*; ASCE: Reston, VA, USA, 1997; pp. 1679–1692.

21. Galland, J.C. Rubble mound breakwater stability under oblique waves: An experimental study. In *Coastal Engineering*; ASCE: Reston, VA, USA, 1995; pp. 1061–1074.
22. Kirkgoz, M.S. Shock pressure of breaking waves on vertical walls. *J. Water Way Port Coast. Ocean Div.* **1982**, *108*, 81–95. [[CrossRef](#)]
23. Kirkgoz, M.S. Breaking wave impact on vertical and sloping structures. *Ocean Eng.* **1995**, *22*, 35–48. [[CrossRef](#)]
24. Liu, Y.L.; Wang, H.F.; Lu, Y. Experimental analysis of the influence of wave period on stability of breakwater armor block. *Coast. Eng.* **2012**, *3*, 364–371.
25. Vicinanza, D.; Contestabile, P.; Nørgaard, J.; Lykke-Andersen, T. Innovative rubble mound breakwaters for overtopping wave energy conversion. *Coast. Eng.* **2014**, *88*, 154–170. [[CrossRef](#)]
26. Christensen, E.D.; Bingham, H.B.; Skou Friis, A.P.; Larsen, A.K.; Jensen, K.L. An experimental and numerical study of floating breakwaters. *Coast. Eng.* **2018**, *137*, 43–58. [[CrossRef](#)]
27. Gürer, S.; Cevik, E.; Yüksel, Y. Stability of tetrapod breakwaters for different placing methods. *J. Coast. Res.* **2005**, *21*, 464–471. [[CrossRef](#)]
28. Verhagen, H.J.; Reedijk, B.; Muttray, M. The effect of foreshore slope on breakwater stability. In *Coastal Engineering 2006*; World Scientific: Singapore, 2007; pp. 4828–4840.
29. Martinelli, L.; Ruol, P.; Volpato, M.; Favaretto, C.; Castellino, M.; De Girolamo, P.; Sammarco, P. Experimental investigation on non-breaking wave forces and overtopping at the recurved parapets of vertical breakwaters. *Coast. Eng.* **2018**, *141*, 52–67. [[CrossRef](#)]
30. Shafieefar, M.; Shekari, M.R.; Hofland, B. Influence of toe berm geometry on stability of reshaping berm breakwaters. *Coast. Eng.* **2020**, *157*, 103636. [[CrossRef](#)]
31. Aniel-Quiroga, Í.; Vidal, C.; Lara, J.L.; González, M.; Sainz, Á. Stability of rubble-mound breakwaters under tsunami first impact and overflow based on laboratory experiments. *Coast. Eng.* **2018**, *135*, 39–54. [[CrossRef](#)]
32. Aniel-Quiroga, Í.; Vidal, C.; Lara, J.L.; González, M. Pressures on a rubble-mound breakwater crown-wall for tsunami impact. *Coast. Eng.* **2019**, *152*, 103522. [[CrossRef](#)]
33. Pillai, K.; Etemad-Shahidi, A.; Lemckert, C. Wave overtopping at berm breakwaters: Experimental study and development of prediction formula. *Coast. Eng.* **2017**, *130*, 85–102. [[CrossRef](#)]
34. Ehsani, M.; Moghim, M.N.; Shafieefar, M. An experimental study on the hydraulic stability of Icelandic-Type berm breakwaters. *Coast. Eng.* **2020**, *156*, 103599. [[CrossRef](#)]
35. Sumer, B.M. Liquefaction around marine structures. In *Proceedings of the Coastal Structures 2007—5th Coastal Structures International Conference, CST07, Venice, Italy, 2–4 July 2007*.
36. Ye, J.H.; Jeng, D.S.; Chan, A.H.C.; Wang, R.; Zhu, Q.C. 3D integrated numerical model for fluid-structures-seabed interaction (FSSI): Loosely deposited seabed foundation. *Soil Dyn. Earthq. Eng.* **2017**, *92*, 239–252. [[CrossRef](#)]
37. Chávez, V.; Mendoza, E.; Silva, R.; Silva, A.; Losada, M. An experimental method to verify the failure of coastal structures by wave induced liquefaction of clayey soils. *Coast. Eng.* **2017**, *123*, 1–10. [[CrossRef](#)]
38. JTS154-1-2011. *Code of Design and Construction of Breakwaters*; Ministry of Transport of China: Beijing, China, 2011. (In Chinese)
39. Department of Army US Army Corps of Engineers. *Coastal Engineering Manual, Engineer Manual 1110-2-1100 (in 6 Volumes)*; Department of Army US Army Corps of Engineers: Washington, DC, USA, 2002.
40. Hughes, S.A. *Physical Models and Laboratory Techniques in Coastal Engineering*; World Scientific: Singapore, 1993.
41. Ikeno, M.; Mori, N.; Tanaka, H. Experimental study on tsunami force and impulsive force by a drifter under breaking bore like Tsunamis. *Coast. Eng. J.* **2001**, *48*, 846–850.